Statistical analysis of turbulent flow over a building array using LES

Osman, Haitham
Interdisciplinary Graduate School of Engineering Sciences, Kyushu University

Muhd Azhar Zainol
Interdisciplinary Graduate School of Engineering Sciences, Kyushu University

Ikegaya, Naoki
Interdisciplinary Graduate School of Engineering Sciences, Kyushu University

https://doi.org/10.5109/7158035

出版情報：Proceedings of International Exchange and Innovation Conference on Engineering & Sciences (IEICES). 9, pp.429-434, 2023-10-19. 九州大学大学院総合理工学府
バージョン：

Statistical analysis of turbulent flow over a building array using LES

Haitham Osman[1*], Muhd Azhar Zainol[1], Naoki Ikegaya[1,2]

[1] Interdisciplinary Graduate School of Engineering Sciences, Kyushu University, Japan
[2] Faculty of Engineering Sciences, Kyushu University, Japan

*Corresponding author email: osman.haitham.413@s.kyushu-u.ac.jp

Abstract: *Understanding the turbulent flow feature over building arrays are essential because the flow distribution is determined by the interaction between the atmospheric boundary layer and building array. The present study investigated the turbulent statistics over roughness elements arranged in a staggered array using large eddy simulation. Unlike a conventional method to drive the flow by the constant pressure gradient, the current simulation method employed a vertical profile of the streamwise pressure gradient determined by the experimental data of the Reynolds stress obtained in a wind tunnel. The time series data were analyzed to determine the fundamental statistics and probabilistic characteristics. The results revealed that the probability density function of the streamwise velocity component followed the gaussian distribution curve behind the building model. However, the probability density function of the vertical component showed a positive skewed results owing to the reverse flow back to the roughness element.*

Keywords: Large eddy simulation; Urban boundary layer; Turbulent statistics

1. INTRODUCTION

Flow over a rough surface obtained much attention from many researchers. Studies investigate the flow characteristics based on wind tunnel experiments, while others studied the flow feature based on numerical simulations, or computational fluid dynamics (CFD). The recent CFD studies determined the instantaneous velocity components by solving Navier–Stokes (NS) equations, although solving the averaged NS equations called Reynolds-averaged NS equations (RANS) to determine the ensemble averaged flow distributions was commonly used. Among these studies dealing with instantaneous velocity, large eddy simulations (LES) solving large eddies numerically and modeling the smaller eddies through sub-grid scale (SGS) models [1] have commonly been used for determining the instantaneous velocity components.

To numerically solve the governing equations described in a Eulerian expression, numerical discretization methods are used such as a finite difference method (FDM) and finite volume method (FVM). Toro [2] explained the discretization process of using the FVM to convert the partial differential equations of fluid flow (continuity and NS equations). Moreover, Felipe et al. [3] recommended using the FVM for unsteady convective fluid flow. Because it is advantageous to generate numerical mesh around complex object.

The steady flow produced by roughness elements would be simulated using RANS equations; however this methodology cannot acquire the instantaneous flow patterns around the roughness blocks [4,5]. Additionally, Castro et al. [6] demonstrated that LES and direct numerical simulation (DNS) can produce a relatively high accurate results to reproduce the velocity components determined by the wind-tunnel experiments. LES technique was also employed in simulating the atmospheric boundary layer [7]. For instance, Vasaturo et al [8] conducted two inlet methods for LES simulations: precursor method and synthetic method (e.g., random number generation and vortex method). The results showed that a precursor method is considered as a suitable way owing to numerical reproduction of the fluid flow in the streamwise direction. Using a precursor LES of the flow inside the wind tunnel, Okaze et al. [9] reproduced the approaching flow through a multiple blocks and the spires of the wind tunnel.

LESs are also employed for many studies dealing with the airflow around blocks and block arrays. For example, Ikegaya et al. [10] performed LES for fluid flow over high rise building. The study demonstrated the statistical flow feature of the turbulent flow over a single block model. Furthermore, Hirose et al. [11] applied LES not only to study the indoor flow feature but also to investigate the thermal comfort in a cross ventilating building. Moreover, Adachi et al. [12] executed LES to examine the sheltering effect from the surrounding building array and to measure the ventilation rate in the cross-ventilation model. In addition, Inagaki et al. [13] studied the turbulence flow structure over a realistic urban geometry numerically using LES. The results explored that the outer-layer features are maintained in the upper portion of the atmospheric boundary layer. Okaze et al. [9] established an LES guidelines by comparing various numerical schemes, mesh resolutions, and turbulence models. Summing up, LES techniques are well established for obtaining an instantaneous velocity distribution around objects such as a building and building arrays.

Although LESs are commonly method, they still require huge computation loads because of the integrating the governing equations in each time step. In addition, sufficient spin-up and calculation periods are required to eliminate the influence of the initial conditions as we as to obtain reliable statistical values. Using a periodic boundary condition for LES in streamwise and spanwise direction is a method to dramatically reduce the simulation costs by mimicking the infinite block arrays streamwise and spanwise directions with a small numerical simulation domain using a momentum source. Xie et al [4] and Coceal et al. [5, 15, 16] employed the flow driving force based on the constant streamwise pressure gradient. However, the output results showed that the change Reynolds shear stress is linear in the vertical direction. Meanwhile, the vertical variation of pressure gradient follows the s-shape profile above the canopy according to the measured data of WTE. Thus, using a constant pressure gradient momentum source would be less realistic while comparing with the quantified Reynolds shear stress from WTE [17, 18].

Under these circumstances, the purpose of this study is to utilize an appropriate momentum source profile to drive airflow over a building array determined by the turbulent statistics measured by a WTE. Accordingly, this study clarifies the statistical and stochastic characteristics of the velocity components by determining the fundamental turbulent statistics and probability density function of the flow around the building array. In Section 2, the numerical method is described, in Section 3 results of turbulent statistics are explained, and Section 4 concludes this study.

2. METHOD

In this section, the governing equation of LES for incompressible turbulent flow will be explained.

The filtered continuity equation is written as

$$\partial_i u_i = 0, \qquad \text{(i)}$$

where u_i represents the grid-scale (GS) streamwise, spanwise, and vertical velocity components for $i = 1, 2,$ and 3, respectively. The corresponding velocity components and coordinates are defined as u, v, w and $x, y,$ and z, respectively. The NS equations are described as

$$\partial_t u_i + \partial_j (u_i u_j) = -\frac{\partial_i p}{\rho} + \partial_j (\tau_{ij} + \nu \partial_j u_i). \qquad \text{(ii)}$$

Here, p is the GS pressure, τ_{ij} denotes the SGS shear stress, and ν is the kinematic viscosity.

The current study utilized the standard Smagorinsky model to parameterize the contribution of the SGS eddies. The SGS stress tensor is defined as shown in equation (3):

$$\tau_{ij} - \frac{1}{3}\tau_{kk}\delta_{ij} = -2\nu_{SGS} S_{ij}, \qquad \text{(iii)}$$

where $S_{ij} = 0.5(\partial_j u_i + \partial_i u_j)$ is the velocity strain tensor, ν_{SGS} is the SGS kinematic viscosity. The SGS kinematic viscosity is modeled as shown in equation (4).

$$\upsilon_{sgs} = (C_s \Delta)^2 S_{ij}, \qquad \text{(iv)}$$

where C_s (=0.12) is the Smagorinsky model coefficient. The length scale Δ is calculated from equation (5).

$$\Delta = \sqrt[3]{\Delta x \Delta y \Delta z} \qquad \text{(v)}$$

Here Δx, Δy, Δz are the grid sizes in each direction. The resolved strain tensor is defined as explained in equations (6) as,

$$|S_{ij}| = \sqrt{2 S_{ij} S_{ij}}. \qquad \text{(vi)}$$

The statistical analysis of the streamwise velocity around a building array model is considered in this study. The array consists of a cube with height of $h = 0.1m$. The roughness elements were arranged in a staggered layout as shown in Figure . The horizontal domain size is $4h \times 4h$, whereas the three heights of the numerical domain, $4h$, $5h$, and $6h$, were investigated. It is worth mentioning that the boundary layer height determined by the WTE data is approximately $5h$.

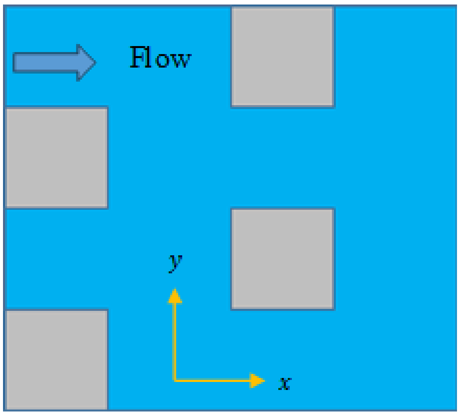

Figure 1. Schematics of the block layout

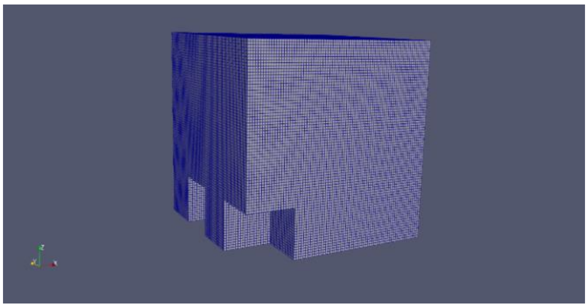

Figure 1. Mesh structures of the numerical

In the proposed method, the momentum source to drive the airflow is determined by the experimental data. The discrepancies between the total momentum, u_τ, provided to the numerical domain and estimated value from the WTE data was approximately 0.7%. The momentum source, equation (7), in the numerical simulation is given via dp/dx, the streamwise pressure gradient to satisfy

$$u_\tau{}^2 = \frac{-1}{\rho}\int_0^{L_z}\frac{dp}{dx}dz. \qquad \text{(vii)}$$

Here, L_z indicate the domain height. The x-y plan view is shown in Figure . The grid size is defined as $h/20$. A mesher implemented in OpenFOAM, snappyHexMesh, was employed to conduct the structured mesh as displayed in Figure 1.

The continuity and the momentum equations were coupled based on the PIMPLE algorithm operated in OpenFOAM. The filteredLinear2V scheme, which blends the linear and upwind interpolation schemes, was employed. More details on the numerical settings are shown in Table 1.

Table 1. Numerical settings

Analysis condition	Numerical setting
Time step	1e-3
Time discretization scheme	Second-order implicit scheme
Sub-grid scale (SGS) model	Smagorinsky model $C_s = 0.12$
Inlet B.C.	Periodic
Outlet B.C.	Periodic
Left B.C.	Periodic
Right B.C.	Periodic
Lower B.C.	Wall (no slip condition)
Upper B.C.	Slip (zero shear stress)
Pre-calculation time	75s
Sampling time	150s

The driving force that provides the momentum source in the computational domain was defined based on the gradient of measured Reynolds shear stress, $\overline{u'w'}$, from wind tunnel experiment using hotwire anemometer (HWA). Here, overbar and prime indicate the temporal average and deviation from the mean.

Figure 2 shows the vertical profile of $\overline{u'w'}$. The maximum value of turbulent shear stress was observed near the top of the roughness element height ($z = 0.1m$). The turbulent shear stress was decreased vertically above the roughness sublayer until the value approaching zero

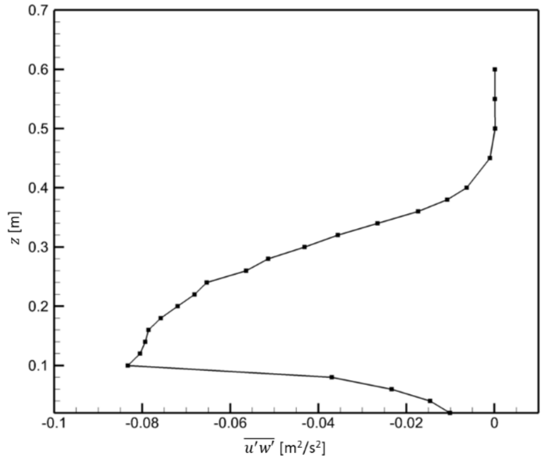

Figure 2. The vertical Reynolds shear stress, $\overline{u'w'}$ obtained in a WTE.

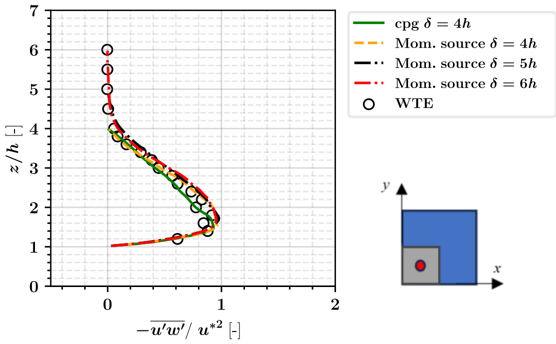

Figure 4. Vertical profile of Reynolds shear stress above the roughness element

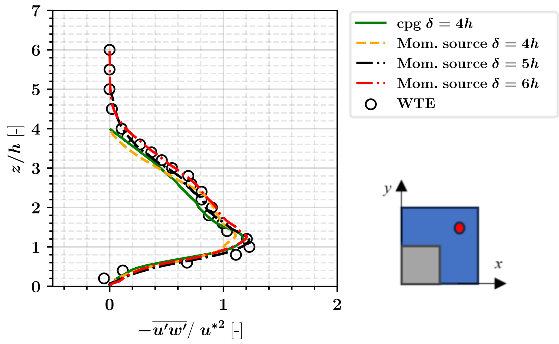

Figure 5. Vertical profile of Reynolds shear stress in front of the roughness element

value above the boundary layer height. In addition, turbulent shear stress is clearly reduced in the canopy layer ($z < 0.1m$) because the effect of form drag acting on the blocks.

The HWA data of $\overline{u'w'}$ was fitted using the error function. Because the vertical slop of $\overline{u'w'}$ determined the momentum source, the normal distribution curve is an empirical function to describe the momentum source.

Using the aforementioned momentum source, three cases with different numerical domain, $\delta = 4h$, $5h$, and $6h$

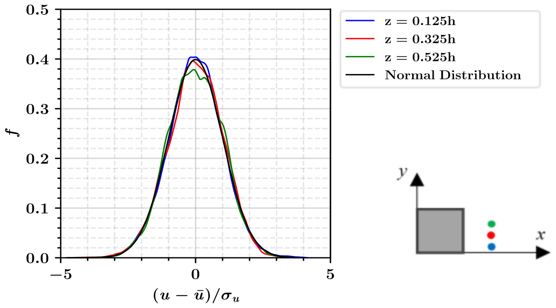

(a) cpg case ($\delta = 4h$)

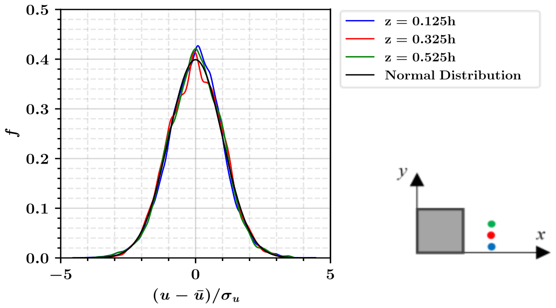

(b) Momentum source case ($\delta = 4h$)

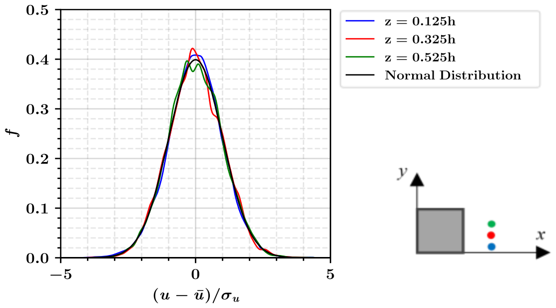

(c) Momentum source case ($\delta = 5h$)

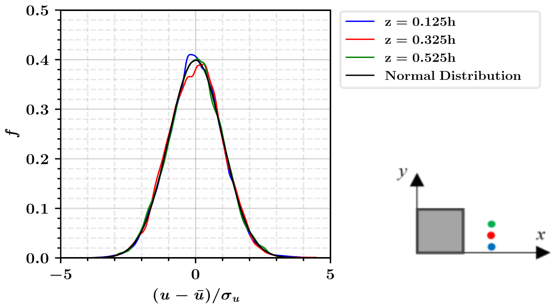

(d) Momentum source case ($\delta = 6h$)

Figure 6. Probability density function for the streamwise velocity component behind the block

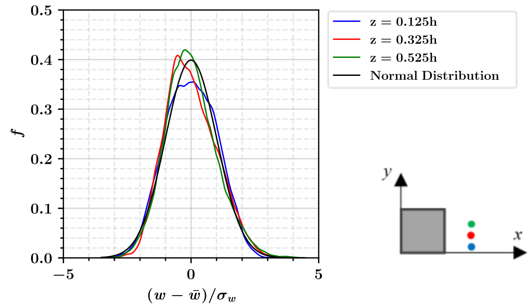

(a) cpg case ($\delta = 4h$)

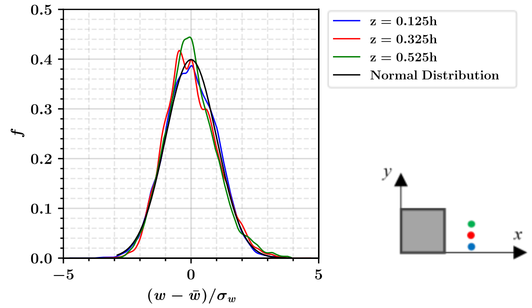

(b) Momentum source case ($\delta = 4h$)

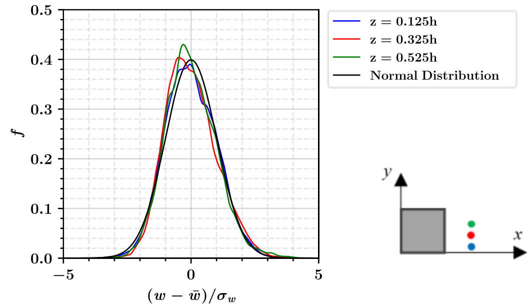

(c) Momentum source case ($\delta = 5h$)

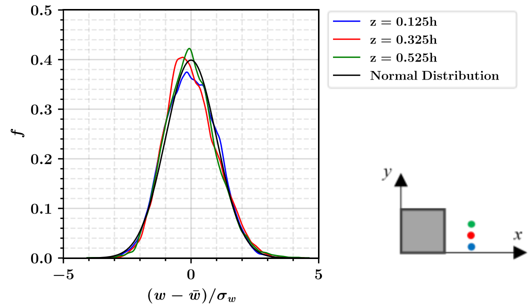

(d) Momentum source case ($\delta = 6h$)

Figure 7. Probability density function for the vertical velocity component behind the block

were investigated. In addition, the results were compared with the constant pressure gradient case denoted as cpg.

3. RESULTS

Figure 4 displays a comparison among three cases with difference boundary layer heights and cpg above a block. The Reynolds stress is normalized by u^{*2} defined by the negative peak values $\overline{u'w'}$. The maximum value was obtained just above the roughness element. For cpg case, the nearly linear reduction of the Reynolds stress with the height is due to the constant driving force in the vertical direction. On the other hand, the other conditions can reproduce the upward convex curve of the Reynolds stress obtained in the WTE.

For the Reynolds stress at a point in front of the block is shown in **Error! Reference source not found.**. It displays a good agreement with each other for four cases and WTE regardless of the driving force and domain height. However, the cases with $\delta = 5h$ and $6h$ can clearly reproduce a slight inflection point around $z = 3h$.

To understand the turbulent flow characteristics, Fig shows the probability density function (PDF), f, of the streamwise velocity component within the wake of the block for cpg case, and three cases with $\delta = 4h$, $5h$, and $6h$. In addition, the Gaussian distribution curve is compared as a reference. The horizontal axis represents a standardized value of the velocity component, where $\overline{u}$ and σ_u represent the mean and standard deviation of u, respectively.

The PDFs at three heights, $z = 0.125h$, $0.325h$ and $0.525h$ are shown in each graph. The differences in the PDFs are very marginal among the four cases; however, the slight differences can be quantified by the statistics shown in Table 2. For cpg case, the PDF of the streamwise velocity at $z = 0.325h$ showed a negatively skewed shape compared with the PDFs for $z = 0.125h$ and $0.525h$, as confirmed by the statistics. The kurtosis of cpg is approximately 3 for three heights, which is consistent with that of the Gaussian distribution. In contrast, the PDFs of the cases with $\delta = 4h$, $\delta = 5h$ and $\delta = 6h$ approximately follow the Gaussian distribution curve at the three observed heights as shown in Figure (b, c, d). These are also confirmed by the statistics in Table 2.

Figure 7 shows the PDFs of the vertical velocity component behind the block element. The PDFs of the vertical component approximately follow the Gaussian distribution as displayed; however, positively skewed shapes can be observed. Table 3 shows the statistics, indicating positively skewed distributions at $z = 0.235h$ and $0.525h$.

Table 2. Skewness and kurtosis of streamwise velocity behind the block at different height.

Case	Statistics	$z = 0.125h$	$z = 0.325h$	$z = 0.525h$
cpg	Skewness	-0.002	-0.169	-0.043
	Kurtosis	3.224	3.030	2.982
$\delta = 4h$	Skewness	-0.052	-0.010	-0.054
	Kurtosis	3.431	2.863	3.288
$\delta = 5h$	Skewness	-0.048	0.045	0.053
	Kurtosis	3.310	3.038	3.046
$\delta = 6h$	Skewness	0.059	0.022	0.002
	Kurtosis	3.318	3.038	3.007

4. CONCLUSION

The present study investigated the effect of the numerical setting on the statistics of the turbulent flow within a canopy of a block array. To accurately reproduce the airflow within and over the array, a pressure gradient profile based on WTE data was employed. Furthermore, the effect of the numerical domain height was also investigated.

The domain height of $\delta = 5h$ and $6h$ can reproduce the Reynolds shear stress obtained by the WTE. The statistical analysis revealed that the PDF approximately follows the Gaussian distribution behind the roughness. However, the PDFs of the streamwise or vertical velocity component behind the block showed negatively or positively skewed shapes.

Table 3. Skewness and kurtosis of vertical velocity component behind the block at different height.

Case	Statistics	$z = 0.125h$	$z = 0.325h$	$z = 0.525h$
cpg	Skewness	-0.015	0.388	0.347
	Kurtosis	2.543	2.851	3.283
$\delta = 4h$	Skewness	0.016	0.317	0.392
	Kurtosis	2.880	2.961	3.357
$\delta = 5h$	Skewness	0.141	0.364	0.331
	Kurtosis	2.929	3.100	3.564
$\delta = 6h$	Skewness	0.066	0.299	0.311
	Kurtosis	2.720	2.940	3.319

5. REFERENCES

[1] N. Ikegaya, T. Kawaminami, T. Okaze, and A. Hagishima, “Evaluation of exceeding wind speed at a pedestrian level around a 1:1:2 isolated block model,” *J. Wind Eng. Ind. Aerodyn.*, 201, (Jun. 2020), 104193.

[2] E. F. Toro, *Riemann Solvers and Numerical Methods for Fluid Dynamics*. Berlin, Heidelberg: Springer Berlin Heidelberg, 2009.

[3] F. A. Díaz, E. Castillo, R. C. Cabrales, and N. O. Moraga, “Non-relaxed finite volume fractional step schemes for unsteady incompressible flows,” *Comput. Math. with Appl.*, 146, (Sep. 2023), 241–252.

[4] Z. Xie and I. P. Castro, “LES and RANS for Turbulent Flow over Arrays of Wall-Mounted Obstacles,” *Flow, Turbul. Combust.*, 76, no. 3, (Apr. 2006), 291–312.

[5] O. Coceal, T. G. Thomas, I. P. Castro, and S. E. Belcher, “Mean Flow and Turbulence Statistics Over Groups of Urban-like Cubical Obstacles,” *Boundary-Layer Meteorol.*, 121, no. 3, (Nov. 2006), 491–519.

[6] I. P. Castro, “Are Urban-Canopy Velocity Profiles Exponential?,” *Boundary-Layer Meteorol.*, 164, no. 3, (Sep. 2017), 337–351.

[7] R. Stoll, J. A. Gibbs, S. T. Salesky, W. Anderson, and M. Calaf, “Large-Eddy Simulation of the Atmospheric Boundary Layer,” *Boundary-Layer Meteorol.*, 177, no. 2–3, (Dec. 2020), 541–581.

[8] R. Vasaturo, I. Kalkman, B. Blocken, and P. J. V. van Wesemael, “Large eddy simulation of the neutral atmospheric boundary layer: performance evaluation of three inflow methods for terrains with different roughness,” *J. Wind Eng. Ind. Aerodyn.*, 173, (Feb. 2018), 241–261.

[9] T. Okaze *et al.*, “Large-eddy simulation of flow around an isolated building: A step-by-step analysis of influencing factors on turbulent statistics,” *Build. Environ.*, 202, (Sep. 2021), 108021.

[10] N. Ikegaya, T. Okaze, H. Kikumoto, M. Imano, H. Ono, and Y. Tominaga, “Effect of the numerical viscosity on reproduction of mean and turbulent flow fields in the case of a 1:1:2 single block model,” *J. Wind Eng. Ind. Aerodyn.*, 191,

(Aug. 2019), 279–296.

[11] C. Hirose, N. Ikegaya, A. Hagishima, and J. Tanimoto, “Indoor airflow and thermal comfort in a cross-ventilated building within an urban-like block array using large-eddy simulations,” *Build. Environ.*, 196, (Jun. 2021), 107811.

[12] Y. Adachi, N. Ikegaya, H. Satonaka, and A. Hagishima, “Numerical simulation for cross-ventilation flow of generic block sheltered by urban-like block array,” *Build. Environ.*, 185, (Nov. 2020), 107174.

[13] A. Inagaki, M. Kanda, N. H. Ahmad, A. Yagi, N. Onodera, and T. Aoki, “A Numerical Study of Turbulence Statistics and the Structure of a Spatially-Developing Boundary Layer Over a Realistic Urban Geometry,” *Boundary-Layer Meteorol.*, 164, no. 2, (Aug. 2017), 161–181.

[14] O. Coceal, A. Dobre, T. G. Thomas, and S. E. Belcher, “Structure of turbulent flow over regular arrays of cubical roughness,” *J. Fluid Mech.*, 589, (Oct. 2007), 375–409.

[15] O. Coceal, T. G. Thomas, and S. E. Belcher, “Spatial Variability of Flow Statistics within Regular Building Arrays,” *Boundary-Layer Meteorol.*, 125, no. 3, (Oct. 2007), 537–552.

[16] H. Cheng and I. P. Castro, “Near Wall Flow over Urban-like Roughness,” *Boundary-Layer Meteorol.*, 104, no. 2, (Aug. 2002), 229–259.

[17] I. P. Castro, H. Cheng, and R. Reynolds, “Turbulence Over Urban-type Roughness: Deductions from Wind-tunnel Measurements,” *Boundary-Layer Meteorol.*, 118, no. 1, (Jan. 2006), 109–131.

[18] S. B. Pope, *Turbulent Flows*. Cambridge University Press, 2000.